Bull. Mater. Sci., Vol. 38, No. 4, August 2015, pp. 1003–1008. © Indian Academy of Sciences.

# Mechanical, dielectric and optical assessment of glass composites prepared using milling technique

**GURBINDER KAUR[1,*], G PICKRELL[1], V KUMAR[2], O P PANDEY[3], K SINGH[3] and S K ARYA[4]**

[1]Department of Material Science and Engineering, Holden Hall, Virginia Tech, Blacksburg, VA 24060, USA
[2]Shri Guru Granth Sahib World University, Fatehgarh Sahib 140 406, India
[3]School of Physics and Materials Science, Thapar University, Patiala 147 004, India
[4]Department of Applied Sciences, ABES Institute of Technology, Ghaziabad 201 009, UP, India

MS received 19 September 2014; accepted 23 March 2015

**Abstract.** **In the present investigation, mechanical and spectroscopic properties of glass composites have been investigated. The glass composites have been prepared by the milling technique instead of using any filler particle. Due to the presence of different alkaline earth modifiers in composites, marked difference in their strength and optical properties is observed. The band gap, Urbach energy and the extinction coefficient of the glass composites have been calculated using UV–visible spectroscopy. Moreover, the real and imaginary dielectric constants have also been calculated for all the composites in addition to the Weibull statistics and cumulative probability of failure. The results have been discussed in light of comparison between the glass composites and the individual glasses. The mechanical and optical properties indicate marked effect on the mechanical strength, band gap and Urbach energy for glass composites as compared with the individual glasses.**

**Keywords.** **Glasses; mechanical properties; optical properties.**

## 1. Introduction

Glasses have many potential applications in electro-optic devices, thermo-mechanical sensors and reflecting windows.[1,2] The properties of glasses are highly sensitive to the composition chosen as the composition determines its local structure.[3–5] The addition of modifier and intermediate oxides can introduce change in the local structure due to variation in interatomic forces. The degree of disorder in glass highly depends upon the nature as well as concentration of modifiers and intermediate oxides. Modifiers like MgO, CaO, SrO and BaO exhibit an observable effect on the optical properties and mechanical properties.

In alkali borosilicate glasses, each alkali atom is surrounded by one non-bridging oxygen (NBO) whereas for alkaline earth borosilicate glasses, two NBOs are present per alkaline earth atom. Therefore, the alkaline earth atoms exhibit stronger structure linkage as compared to the alkali atoms, hence leading to the immobilization of alkaline modifier atom. Such glasses containing alkaline earth metal ions posses higher chemical durability.[6] Researchers in our group have investigated the optical properties of lanthanum borosilicate glasses during our previous studies.[7] Lanthanum oxide ($La_2O_3$) generally acts as an intermediate in glass composition and enhances the chemical durability as well as the optical properties.[8] In the present studies, the optical and mechanical properties of glass composites prepared using a novel approach of milling have been investigated, i.e., instead of incorporating the unreactive particles in a glass matrix, the glasses have been mixed in fixed ratio and then ball milled for 5 h.[9] The composite of two glassy materials is chemically more compatible to each other, and a uniform and homogenized glass composite could be obtained by high-energy ball milling, which could further help in improving particle size hence influencing its strength and band-gap. The glass composites prepared by this methodology have more than one alkaline earth modifier without using any filler material. The alkaline earth oxides break the B–O–B bonds leading to compactness of structure hence exhibiting marked effect on the properties.[10] Based on these objectives, the properties of glass composites were investigated using UV–vis and microhardness tester. In addition to this, hardness and indentation toughness of glass composites are analysed using the statistical aspect. Study of optical properties was carried out thoroughly and structure–properties correlation was established. Furthermore the band gap, Urbach energy, hardness and fracture toughness have been compared for glass and glass composites.

## 2. Experimental

The glasses were prepared by taking required stochiometric amounts of different constituent oxides or carbonates of 99.9% purity. These constituents were first mixed together using ball mill in acetone medium. The powder obtained after ball milling was melted at 1550°C in high resistance furnace.

*Author for correspondence (gkaur82@vt.edu)

The melt was quenched in air using copper plates. The quenched glass was annealed at 500°C in preheated furnace to remove the internal stresses from the glasses. The preparation details of the ML, CL, SL and BL glasses chosen for making composites are given elsewhere and the compositions are listed in table 1.[11,12] Furthermore, different glass compositions were mixed in ratio 1:1 and then ball milled for 5 h to obtain composites.[9] The composites obtained are listed in table 2 along with their sample labels.

The optical transmission spectra of the prepared samples were recorded at room temperature using a double beam, UV–vis spectrophotometer (Model: Perkin Elmer Lambda 45) in the wavelength range of 200–700 nm. Methanol was taken as the reference solution. The spectrum of each sample was normalized to the spectrum of the blank methanol. LECO LM247AT Microhardness Tester and Control Software are used for measuring microhardness of the samples.

## 3. Results

### 3.1 *Absorption studies and refractive index*

The optical properties of materials are always governed by the interaction between solid and electromagnetic radiations. Optical absorption is related to transmittance by following relation:[13]

$$\alpha = (2.303/d)\log(1/T). \tag{1}$$

Figure 1 gives the plots for absorption ($\alpha$) *vs*. wavelength ($\lambda$) for all the samples in UV–vis optical absorption region. The absorption edges are sharply defined indicating the crystalline nature of samples. The absorption follows the trend GG5 > GG6 > GG7 > GG1 > GG2 > GG3 > GG4. The transmission spectra follow the reverse order for samples as depicted by figure 2. The absorption coefficient ($\alpha$) is also related to extinction coefficient ($k$) as follows:

$$\alpha = 4\pi k/\lambda \tag{2}$$

$k$ is generally related to decay or damping of oscillation amplitude of incident electric field. The variation of $k$ with wavelength for all the composites is shown been figure 3a. According to the theory of reflectivity of light, the refractive index $n$, as a function of the transmission measurements is determined by Fresnel's equations

$$R = \left[(n-1)^2 + k^2\right] / \left[(n-1)^2 + k^2\right]. \tag{3}$$

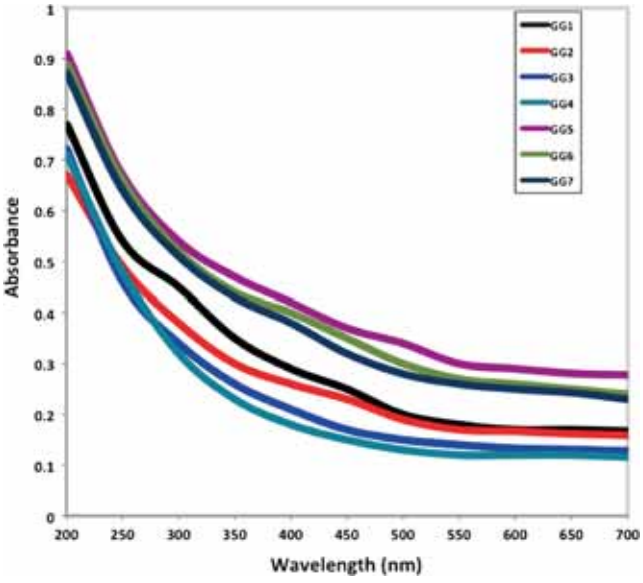


**Figure 1.** Absorption spectra of all the glass composites.

**Table 1.** Glass composition along with sample labels.[6]

| Glass | MgO | CaO | SrO | BaO | $SiO_2$ | $B_2O_3$ | $La_2O_3$ |
|---|---|---|---|---|---|---|---|
| ML | 30 | 0 | 0 | 0 | 40 | 20 | 10 |
| CL | 0 | 30 | 0 | 0 | 40 | 20 | 10 |
| SL | 0 | 0 | 30 | 0 | 40 | 20 | 10 |
| BL | 0 | 0 | 0 | 30 | 40 | 20 | 10 |

**Table 2.** Direct/indirect band gap ($E_{opt}$), Urbach energy ($E_u$), hardness ($H$), fracture toughness ($K$) and Weibull parameters of all composite samples.

| Sample name | Composition (1:1) | Direct $E_{opt}$ (eV) ± 0.01 | Indirect $E_{opt}$ (eV) ± 0.01 | $E_u$(eV) ± 0.001 | $H$ (GPa) ± 0.01 | $K$ (MPa $m^{1/2}$) ± 0.01 | $K_o$ (MPa $m^{1/2}$) ± 0.001 | $m$ ± 0.01 |
|---|---|---|---|---|---|---|---|---|
| GG1 | ML+ CL | 3.16 | 2.69 | 0.627 | 9.67 | 3.42 | 1.901 | 13.11 |
| GG2 | CL+SL | 3.12 | 2.57 | 0.648 | 8.93 | 3.28 | 1.133 | 15.01 |
| GG3 | SL+BL | 2.44 | 1.62 | 0.671 | 8.62 | 3.01 | 0.516 | 11.87 |
| GG4 | BL+ML | 3.01 | 2.34 | 0.638 | 8.88 | 3.31 | 1.416 | 16.46 |
| GG5 | BL+CL | 2.79 | 2.14 | 0.674 | 8.53 | 2.96 | 0.637 | 19.81 |
| GG6 | ML+SL | 3.08 | 2.51 | 0.662 | 8.57 | 2.89 | 1.815 | 12.19 |
| GG7 | ML+CL+SL+BL | 2.72 | 1.97 | 0.687 | 8.78 | 3.09 | 2.341 | 13.95 |

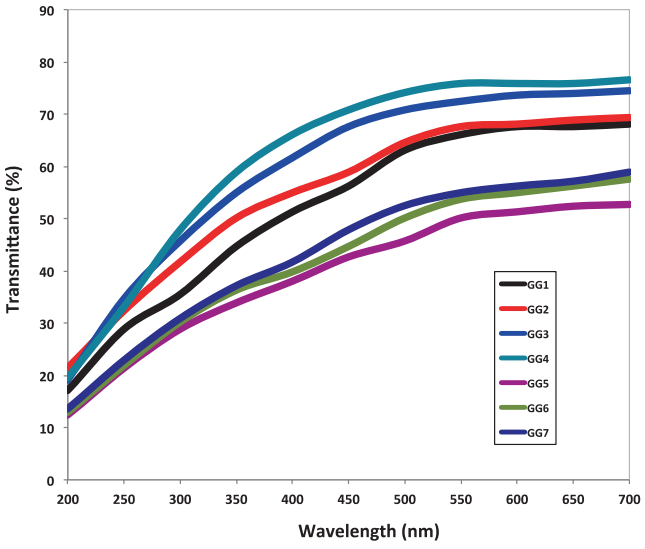


**Figure 2.** Transmission spectra of all the glass composites.

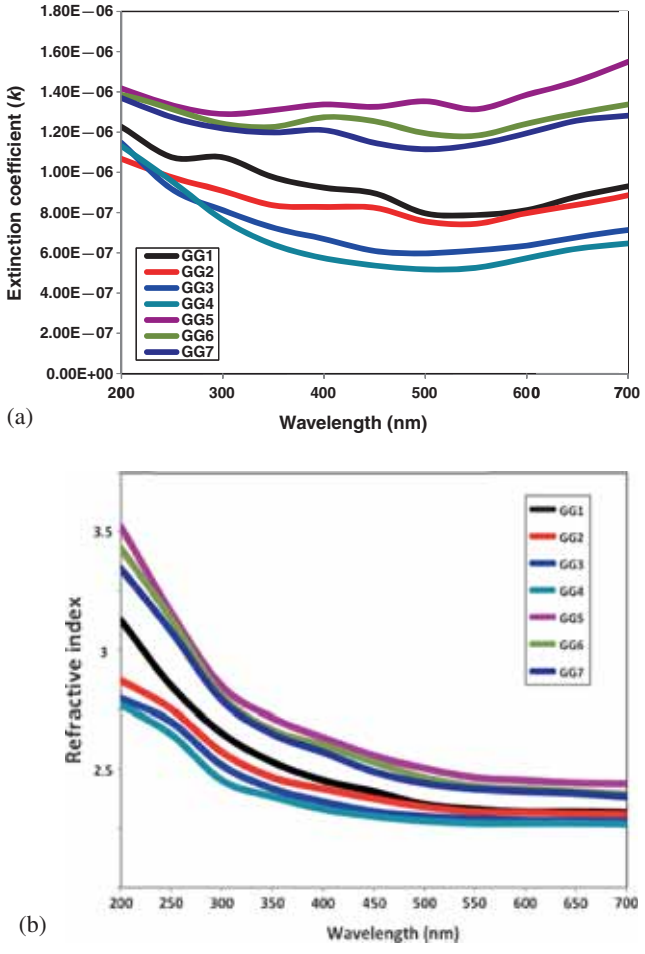


**Figure 3.** (**a**) Extinction coefficient for all the glass composites and (**b**) refractive index variation of all the glass composites.

It is clear from figure 3b that the refractive index decreases with an increase in the wavelength of the incident photon. Refractive index decreases with the increase in wavelength and follow the trend GG5 > GG6 > GG7 > GG1 > GG2 > GG3 > GG4. Hence, the sample with high transmission has small refractive index. The variation of refractive index can be explained on the basis of Lorentz–Lorenz equation as follows. The co-ordination number also affects the refractive index. BaO is a strong modifier in comparison to MgO, CaO and SrO. It creates more NBOs which in turn increases the average co-ordination number of glasses. Modifier ions will act partly as bridges between network forming groups and partly enclosed within the structural interstices. This position is the least stable position and is known as ionic bridging position.[14]

The optical properties of a medium are also characterized by the complex refractive index ($N$) and complex dielectric constant ($\varepsilon$) given by following equations:[15]

$$N = n - \mathrm{i}k, \tag{4}$$

$$\varepsilon = \varepsilon_\mathrm{i} - \mathrm{i}\varepsilon_0, \tag{5}$$

$\varepsilon_\mathrm{i}$ and $\varepsilon_0$ represent in the phase and out of phase components of the frequency response for medium, respectively. The real in phase component usually contributes to the refraction of electromagnetic radiation when it passes through the medium. The imaginary out of phase component represents absorption via the following three mechanisms: (i) visible electronic state transitions, (ii) infrared vibrational transitions and (iii) microwave rotational transitions. Complex refractive index and dielectric constant are related to each other as $\varepsilon = N^2$. Hence, we obtain the following relations implementing real and imaginary dielectric coefficients:

$$\varepsilon_\mathrm{i} = n^2 - k^2, \tag{6}$$

$$\varepsilon_0 = 2nk. \tag{7}$$

Figure 4a and b represents the variation of real and imaginary dielectric constants with wavelength for all the samples. All the composite samples have shown an increase in real dielectric constant with wavelength whereas the imaginary dielectric constant decreases with wavelength. The real dielectric constant follows the trend GG5 > GG6 > GG7 > GG1 > GG2 > GG3 > GG4. The imaginary dielectric constant also follows the same trend, i.e., GG5 > GG6 > GG7 > GG1 > GG2 > GG3 > GG4 which goes in accordance with the absorption spectra (figure 1).

### 3.2 *UV–vis spectroscopy*

For in-depth analysis of band structure, optical measurements are very productive tools. During optical absorptions, the photons are absorbed either by lattice phonons or electrons. The phonon absorption gives information about atomic vibrations, which is usually in infrared region of spectrum.[16] Inter-band electronic transitions belong to higher energy parts of spectrum and give information about electronic states. During these transitions, a considerable sharp increase in absorption coefficient results due to excitation of electrons from filled to empty band by phonon absorption. This

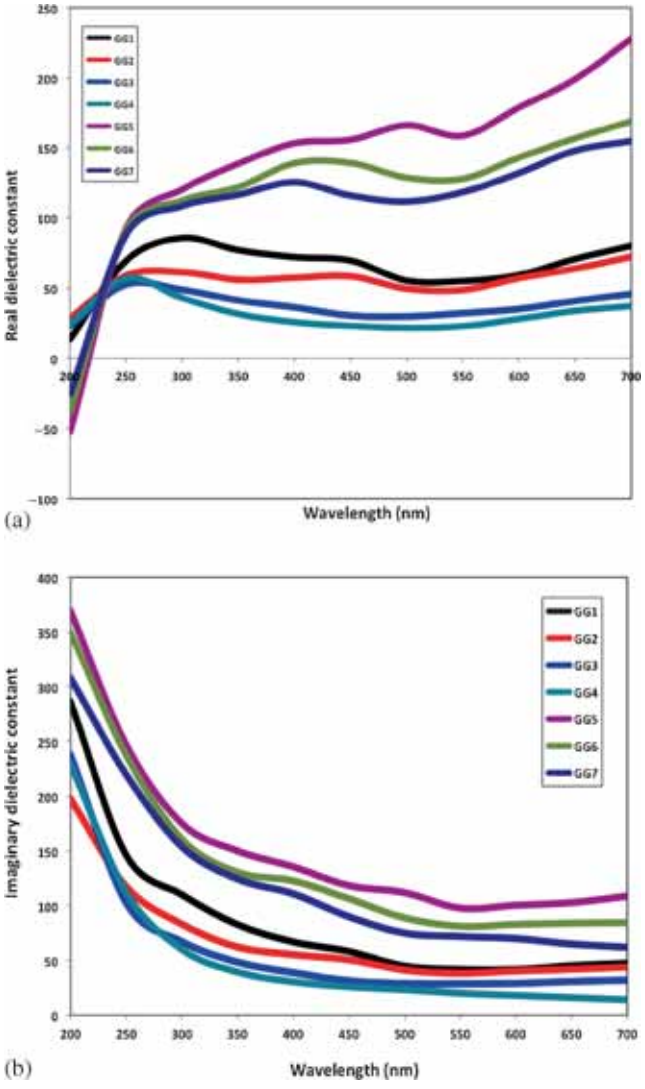


**Figure 4.** (**a**) Real dielectric constant of all the glass composites and (**b**) imaginary dielectric constant of all the glass composites.

onset of marked increase in absorption is designated as the fundamental absorption edge. The oxide ion contains modifier ions which play a very important role in describing absorption processes, i.e., internal transitions among d-shell electrons and absorption due to transfer of an electron from neighbouring atom to modifier ion and vice-versa. The fundamental transitions include interaction of electromagnetic radiation with an electron in the valence band. During direct optical transitions, the wave vector for the electron is unchanged. During indirect transitions, the wave-vector of the electron can change and momentum is also changed, but the conservation of momentum follows.

The absorption coefficient for the Tauc region (region of inter-band transitions) is given in quadratic form by Mott and Davis[17] in more general form as follows:

$$\alpha h\nu = B\left[\frac{\left(h\nu - E_{\text{opt}}\right)^n}{h\nu}\right], \tag{8}$$

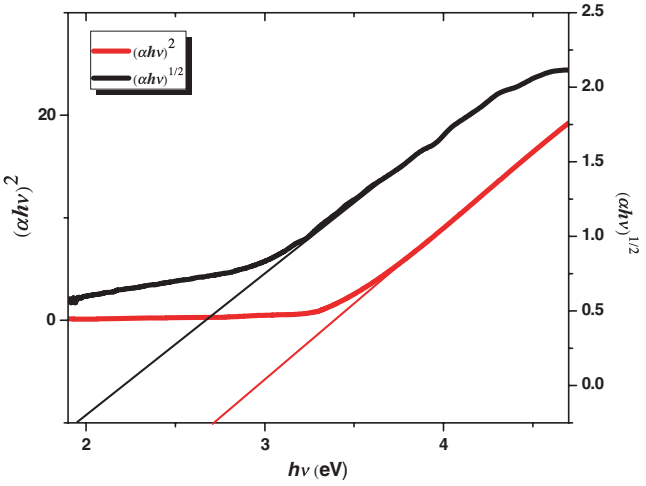


**Figure 5.** Direct and indirect band gap of sample GG7.

where $B$ is the constant which depends upon transition probability, $h\nu$ the photon energy and $E_{\text{opt}}$ the optical band gap related to energy gap between valence band and conduction band. Here, $n$ is an index, which characterizes the optical absorption process. Exponent $n$ can have four values: 2, 1/2, 3, 3/2 representing indirect allowed, direct allowed, indirect forbidden and direct forbidden.[18,19] Plots of $(\alpha h\nu)^{1/n}$ *vs.* incident photon energy h$\nu$ are used to determine the type of optical transition. The plots for $(\alpha h\nu)^2$ and $(\alpha h\nu)^{1/2}$ *vs.* $h\nu$ is plotted in figure 5 for sample GG7. $E_{\text{opt}}$ values are determined by extrapolating the linear region of the plots to $(\alpha h\nu)^2$ and $(\alpha h\nu)^{1/2} = 0$. The values of direct and indirect $E_{\text{opt}}$ are listed in table 2.

Direct band gaps are larger than indirect band gaps for all the samples. The plots that satisfy the widest linearity of data determine the dominant transitions. According to this criterion, direct allowed transitions dominate in the present case. Sample GG1 has highest direct as well as indirect band gap. In addition to this, sample GG3 has lowest band gap. Variation in optical band gap is also attributed to different structural cations present in the network. For the present samples, it is attributed to the network structural differences introduced due to the different modifier atoms. It can be seen from table 2, that the band gap is small for the samples having higher atomic mass modifier atoms like $Sr^{2+}$ and $Ba^{2+}$. Their introduction would cause the Si–O–Si bonds breakage and creates appearance of non-bridging oxygens (NBO) in the network.[20] Shift of energy gap to lower energies can be due to the formation of NBOs. It is well reported in the literature that the introduction of heavy metals like barium in glass composition decreases the optical band gap.[7]

The Urbach energy in the tail region where $\alpha(\nu)$ depends exponentially on the photon energy $h\nu$ is given as follows:[21]

$$\alpha(\nu) = \alpha_0 \exp\left(h\nu/E_u\right), \tag{9}$$

where $\alpha_0$ is a constant and $E_{\text{u}}$ the Urbach energy indicating the width of band tails of localized states representing degree

of disorder. Urbach energy measures the degree of disorder for amorphous/crystalline materials.[22,23] $E_u$-values are calculated from slopes of linear portion of the curve between $\ln(\alpha)$ against $h\nu$ and are tabulated in table 2. Urbach energy is highest for sample GG7 and it is lowest for sample GG1. This indicates that the sample GG7 having all the modifiers possess more structural randomness. The third region is the weak absorption tail produced from defects and impurities in UV spectra.

When compared to the results of our previous work,[7] the direct band gap has been higher for all the composites except GG3 than the band gap of individual glasses, i.e., the direct band gap for the glass composites lie in the range of 2.44–3.16 whereas that of glasses lie in the range 2.02–2.64. Similar results have been obtained for the Urbach energy also, where the degree of randomness is more for glass composites as compared to individual glasses. The Urbach energy for the glass composites lie in the range of 0.627–0.687 and that of individual glasses lie in the range of 0.34–0.47. Lower $E_{opt}$-values for GG7, GG5 and GG3 samples indicate the formation of more NBOs in them and hence increased amorphousicity or structural randomness of the samples. The increased structural randomness is also evident from high Urbach energy of GG7 sample followed by GG5 and GG3 samples.

### 3.3 *Microhardness testing and cumulative distribution function*

The hardness and indentation fracture toughness for all the samples are listed in table 1. Hardness ($H$) and fracture toughness ($K$) for the glass composites have been obtained using the following relations:[24,25]

$$H = F/A \approx 1.8544F/d^2,$$
$$K = 0.016(E/H)^{1/2}(F/c^{3/2}), \quad (10)$$

where $F$ is the indentation load, $d$ the diagonal length of indentation and $c$ the half-length of the resultant indentation cracks, $E$ and $H$ Young's modulus and the hardness of the test materials, respectively. An elastic modulus ($E$) of 200 GPa is used for calculating fracture toughness.[26,27] Cumulative probability of failure ($P_i$) for 50 K points has been calculated[7] using cumulative distribution function (CDF). $P_i$ is assigned to the $i$th result of $(K_c/K_{av})_i$ and is given by Gong as follows:[28]

$$P_i = (i - 0.5)/50. \quad (11)$$

The shape of the CDF obtained in figure 6a is in correlation with those generally observed for the brittle ceramics.[7] The fracture behaviour of brittle materials is described using Weibull statistics.[29] Weakest-link hypothesis states that the most severe flaw controls the strength of the materials. Under an applied stress $K$, the cumulative probability of failure for a brittle material can be expressed as

$$P_i = 1 - \exp[-(K/K_o)^m], \quad (12)$$

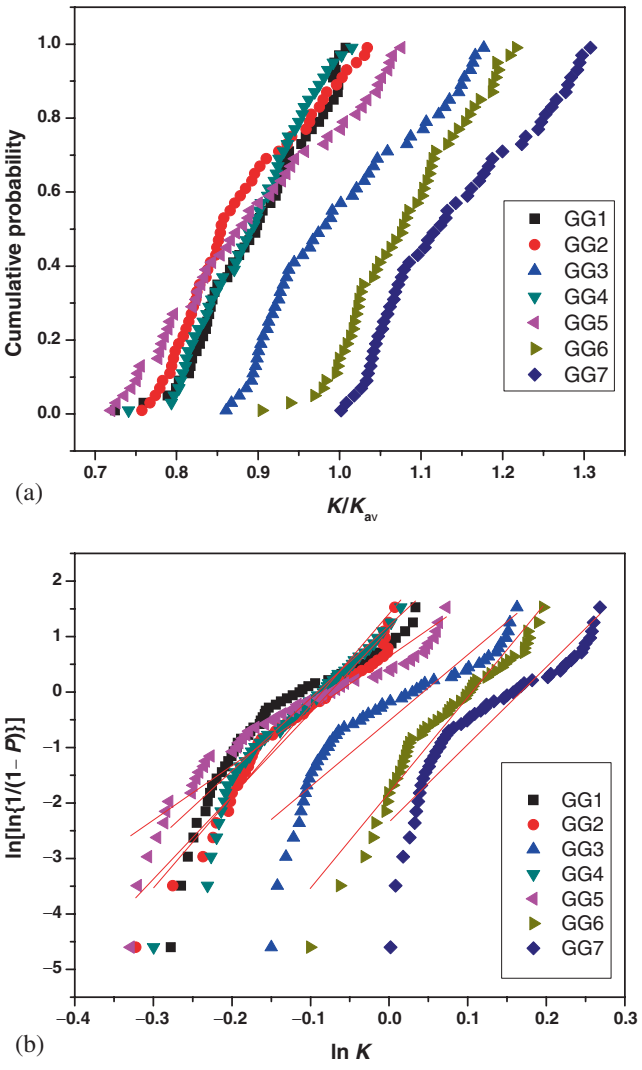


**Figure 6.** (**a**) Cumulative probability of failure for all the samples and (**b**) Weibull plots for fracture toughness of all the samples.

where $K_o$ is the Weibull characteristic strength and $m$ the Weibull modulus, measures the degree of data dispersion. Briefly, 50 data points for Weibull analysis have been generated for each sample and are depicted in figure 6b. $K_o$ and $m$ are estimated with the conventional least-square fitting method. The obtained results are summarized in table 2. It can be observed from table 2, that GG1 sample has maximum hardness as well as fracture toughness. The reason can be attributed to the bond strength pattern which varies as MgO > CaO > SrO > BaO.[30] GG1 sample has MgO and CaO, hence much attraction between bonds. Low values of $K$ and $K_o$ for samples GG3 and GG5 can be attributed to the lower bond strength for BaO oxide as compared with SrO and CaO oxides. The characteristic Weibull strength $_{Ko}$ is also highest for GG1 sample, which can be due to its high bond strength. Weibull modulus is highest for GG5 sample and low for GG3 sample indicating high data dispersion in GG5 sample. Furthermore, GG5 sample exhibits lowest value for hardness as well as fracture strength. From

our previous studies,[7] it can be observed that the hardness and fracture toughness for all the glass composites is high as compared to individual glasses. In addition to this, maximum Weibull strength of 2.341 is obtained for GG7 composite which is higher than any of the individual glass. The above study clearly indicates that modifiers influence the basic property of glasses. Also, the composites have shown enhanced mechanical properties as compared to individual glasses.

## 4. Conclusions

Different modifiers can exhibit a strong effect on mechanical, structural and optical properties of composites. The glass composites containing barium show a decrease in optical band gap decreases due to an increase in the number of non-bridging oxygen. GG7 composite shows maximum Urbach energy due to the structural randomness attributed to four modifier atoms. GG5 sample shows maximum absorption whereas GG4 gives maximum transmittance. The real dielectric constant follows the trend GG4 > GG3 > GG2 > GG1 > GG7 > GG6 > GG5, whereas the imaginary dielectric constant follows reverse trend. GG1 sample possesses the highest hardness and fracture strength, which is due to MgO and CaO in its composition, hence higher bond strength. GG5 sample gives maximum data dispersion, which is evident from its high Weibull parameter along with low fracture strength. The composites have shown enhanced mechanical as well as optical properties as compared to individual glasses.

## Acknowledgements

We are thankful to CIES, Washington D.C. for financial assistance. Also thankful to Dr D Homa and Dr B Scott, Virginia Tech, for their help and cooperation throughout the studies.

## References

1. Hall D W, Newshouse M A, Borelli N F, Dumbaugh W H and Weidmann D L 1989 *Appl. Phy. Lett.* **54** 1293
2. Kaur G, Kumar M, Arora A, Pandey O P and Singh K 2011 *J. Non-Cryst. Solids* **357** 858
3. Subbalakshmi P and Veeraiah N 2002 *J. Non-Cryst. Solids* **298** 89
4. Manupriya K, Thind S, Sharma G, Rajendran V, Singh K, Gayathri Devi A V and Aravindan S 2006 *Phys. Status Solidi A* **203** 2356
5. Sharma G, Thind K S, Singh M H and Gerward M L 2007 *Phys. Status Solidi A* **204** 591
6. Raghvan V 2008 Materials science and engineering (New Delhi: PHI Learning Pvt. Ltd.) p 81
7. Kaur G, Pandey O P and Singh K 2012 *J. Non-Cryst. Solids* **358** 2589
8. Singh K, Bala I and Kumar V 2009 *Ceram. Int.* **35** 3401
9. Kaur G, Singh K, Pandey O P, Homa D, Scott B and Pickrell G 2013 *J. Power Sources* **240** 458
10. Sebastian S and Khadhar M A 2005 *J. Mater. Sci.* **40** 1655
11. Kaur G, Pandey O P and Singh K 2012 *Int. J. Hydrogen Energy* **37** 6862
12. Kaur G, Pandey O P and Singh K 2012 *Int. J. Hydrogen Energy* **37** 3883
13. Abdel-Baki M, Abdel Wahab F A and El-Diasty F 2006 *Mater. Chem. Phys.* **96** 201
14. Baki M A, Wahab F A A, Radi A and Diasty F E 2007 *J. Phys. Chem. Solids* **68** 1457
15. Rajesh K R and Menon C S 2002 *Mater. Lett.* **53** 329
16. El-Deen L M S, Salhi M S and Elkoholy M M 2008 *J. Alloys Compd.* **465** 333
17. Mott N F and Davis E A 1979 *Electronic processes in non-crystalline materials* (Oxford: Clarendon) p 287
18. Mirzayi M and Hekmatshoar M H 2009 *Ionics* **15** 121
19. Shakeri M S and Rezvani M 2011 *Spectrochim. Acta A* **79** 1920
20. Duffy J A and Ingram M D 1976 *J. Non-Cryst. Solids* **21** 373
21. Urbach F 1953 *Phys. Rev.* **92** 1324
22. Saito K and Ikushima A 2000 *J. Phys. Rev. B* **62** 8584
23. Redfield D 1963 *Phys. Rev.* **130** 916
24. Anstis G R, Chantikul P, Lawn B R and Marshall D B 1981 *J. Am. Ceram. Soc.* **64** 533
25. Nilihara K, Morena R and Hasselman D P H 1982 *J. Mater. Sci. Lett.* **1** 13
26. Adams J W, Ruh R and Mazdiyasni K S 2005 *J. Am. Ceram. Soc.* **80** 903
27. Kaur G, Pandey O P and Singh K 2012 *Phys. Status Solidi A* **209** 1231
28. Gong J 2002 *Ceram. Int.* **28** 767
29. Richerson D W 1992 *Modern ceramic engineering* (New York, USA: Marcel Dekker, Inc.) 2nd ed
30. Ghosh S, Kundu P, Sharma A D, Mahanty S and Basu R N 2008 *J. Non-Cryst. Solids* **354** 4081